

## Parton-transverse-momentum effects and the quantum-chromodynamic description of high- $p_T$ processes

J. F. Owens and J. D. Kimel

*Physics Department, Florida State University, Tallahassee, Florida 32306*

(Received 28 March 1978)

Previous calculations have shown that quantum chromodynamics can successfully describe the behavior of high- $p_T$  single-particle inclusive processes in the region  $\sqrt{s} \gtrsim 50$  GeV and  $p_T \gtrsim 5$  GeV/c. Here it is shown that this region can be enlarged significantly by including effects due to parton transverse momenta.

### I. INTRODUCTION

In the last year much work has been focused on obtaining a quantitative description of high- $p_T$  inclusive processes in the context of quantum chromodynamics (QCD). The results of these calculations<sup>1-3</sup> show that, indeed, QCD is capable of describing these processes subject to the constraints  $\sqrt{s} \gtrsim 50$  GeV and  $p_T \gtrsim 5$  GeV/c. These limitations have left open the possibility that some alternative mechanism may be operating at lower energies and/or  $p_T$ . Each of these early calculations had in common the use of purely longitudinal parton distributions. However, data for two-particle inclusive reactions have shown that the average parton transverse momentum is rather large.<sup>4</sup> A similar conclusion has been reached on the basis of the large average transverse momentum of dimuon pairs observed in hadronic dimuon production.<sup>5,6</sup> These observations have led various groups to study the effects on high- $p_T$  calculations of including parton-transverse-momentum effects. This problem has been studied both with phenomenological models<sup>4,7,8</sup> and QCD calculations.<sup>9</sup> In each instance the conclusion has been that parton transverse momenta can cause a significant enhancement of the invariant cross section in the intermediate  $p_T$  range  $2 \lesssim p_T \lesssim 4$  GeV/c.

In Ref. 3 detailed QCD predictions were given for the  $p_T$  and angular dependences of single-particle, high- $p_T$ , inclusive cross sections and for particle production ratios. In this analysis the effects of parton transverse momenta on these observables will be presented. In addition, the previous calculations have been modified by including a more precise treatment of the  $Q^2$  dependence of the parton fragmentation functions.<sup>10</sup> In Sec. II the various parton distribution and fragmentation functions and subprocess expressions are reviewed. Here, too, the method of treating the parton transverse momenta is presented. In Sec. III the results of this calculation are compared with available data and the conclusions are presented in Sec. IV.

### II. CROSS-SECTION CALCULATIONS

In calculations of high- $p_T$  cross sections, three distinct pieces of input are required: (a) the parton distribution functions, (b) the expressions for the parton-parton interaction cross sections, and (c) the parton fragmentation functions. In this section each of these three items will be briefly reviewed and the necessary modifications for the inclusion of parton-transverse-momentum effects will be noted.

#### A. Distribution functions

The parton distribution functions used in this analysis have been obtained by first fitting simple functional forms to leptonproduction data<sup>11,12</sup> for  $Q^2 = Q_0^2 = 4$  (GeV/c)<sup>2</sup>. A conventional valence-sea decomposition was assumed and the input parametrization followed that of Ref. 13:

$$x[u_v(x, Q_0^2) + d_v(x, Q_0^2)] = \frac{3}{B(\eta_1, 1 + \eta_2)} x^{\eta_1} (1 - x)^{\eta_2}, \quad (1)$$

$$x d_v(x, Q_0^2) = \frac{1}{B(\eta_3, 1 + \eta_4)} x^{\eta_3} (1 - x)^{\eta_4}, \quad (2)$$

$$x s(x, Q_0^2) = 6 x s(x, Q_0^2) = A_s (1 - x)^{\eta_s}, \quad (3)$$

$$x g(x, Q_0^2) = A_g (1 - x)^{\eta_g}, \quad (4)$$

where the Euler beta functions,  $B(\eta_i, 1 + \eta_{i+1})$ , are used to ensure baryon-number conservation. The fitted parameter values are

$$\eta_1 = 0.624, \quad \eta_2 = 2.657, \quad \eta_3 = 0.773$$

$$\eta_4 = 3.70, \quad A_s = 1.053, \quad \text{and } \eta_s = 8.$$

For the gluon distribution  $\eta_g = 5$  was assumed in accordance with counting rules<sup>14</sup> and  $A_g = 2.676$  was fixed by momentum conservation. For  $Q^2 = Q_0^2$  it was assumed that the charm sea was zero; the  $Q^2$  dependence introduced by the QCD scaling violations will then produce a charm sea for higher  $Q^2$ . However, this will not play a role in the present analysis.

The values of the moments of the input parton

distribution functions at  $Q^2 = Q_0^2$  may be obtained by Mellin transforming the expressions given in Eqs. (1)–(4). The moments for  $Q^2 > Q_0^2$  are then determined by the input moments once the QCD scale parameter  $\Lambda$  is specified.<sup>15</sup> This parameter determines the strength of the strong running coupling constant and, hence, sets the scale for the  $Q^2$  dependence of the moments. In the one-loop approximation the leading logarithm expression for  $\alpha_s$  is<sup>15</sup>  $\alpha_s = 12\pi/(33-2N)\ln(Q^2/\Lambda^2)$ , where  $N$  is the number of quark flavors. The  $Q^2$ -dependent moments may then be Mellin-inverted to obtain the  $Q^2$ -dependent parton distribution functions. The above procedure was performed and the resulting functions were compared with the data in order to obtain an estimate for  $\Lambda$ ; a preferred value of 0.4 was found, in agreement with Ref. 16.

It is the purpose of this analysis to investigate the possible effects of parton transverse momenta in high- $p_T$  hadronic collisions. Accordingly, the parton distribution functions must be modified to accommodate a dependence on the parton transverse momentum,  $\vec{k}_T$ . Denote the distribution function for a parton  $a$  in a hadron  $A$  by  $G_{a/A}(x_a, \vec{k}_T, Q^2)$ . Hereafter, the  $Q^2$  dependence will not be explicitly stated. For the purpose of this calculation a simple factorized form has been assumed for the  $\vec{k}_T$  dependence,

$$G_{a/A}(x_a, \vec{k}_T) = \frac{A_a}{\pi} G_{a/A}(x_a) e^{-A_a k_T^2}, \quad (5)$$

where the normalization has been chosen such that

$$G_{a/A}(x_a) = \int d^2k_T G_{a/A}(x_a, \vec{k}_T). \quad (6)$$

The factorized form shown in Eq. (5) is likely to be an oversimplification and, in general,  $A_a$  could possess both  $x$  and  $Q^2$  dependence. Indeed, QCD arguments suggest that several effects are present. First, the partons should have some intrinsic transverse momenta as a result of being confined inside the parent hadron. Second, there are effects from higher-order diagrams involving, for example, gluon bremsstrahlung. To leading order in  $\ln Q^2$  these latter effects are included in the calculation when  $Q^2$ -dependent parton distribution functions are used.<sup>17</sup> However, there are additional contributions from wide-angle emission which give rise to recoil effects. In this case the outgoing observed hadron comes from a parton which is recoiling against a hard gluon. Higher-order effects such as these thus alter the observed  $p_T$  distribution by smearing it outwards towards higher  $p_T$  values.<sup>18</sup> If both of these effects are combined to give an effective  $k_T$  distribution, then a form such as

$$\langle k_T^2 \rangle = a + b\alpha_s(Q^2)Q^2 \quad (7)$$

would be more realistic. Here  $a$  is a constant which reflects the intrinsic  $k_T$  distribution and  $b$  is a function of  $x$  and  $Q^2/s$  which can be calculated for a given process in QCD.<sup>20</sup>

In light of the above discussion, Eq. (5) represents at best an average  $k_T$  distribution which results from several sources. Nevertheless, at this state Eq. (5) can serve as a useful phenomenological approximation with which one can explore the consequences of including parton-transverse-momentum effects. Recall, too, that the “smearing” introduced by the parton transverse momenta is appreciable only in a limited kinematic region.<sup>7</sup> For example, at  $\sqrt{s} = 53$  GeV this region is limited to  $\langle Q^2 \rangle \lesssim 100$  (GeV/c)<sup>2</sup> and  $\langle x \rangle \lesssim 0.4$ . The assumption of a constant value for  $\langle k_T^2 \rangle$  over this range is, therefore, not too severe.

Before proceeding further it is necessary to obtain some estimate for the parameter  $A_a$  for each of the different types of partons. An initial estimate may be obtained using dimuon production data.<sup>5,6</sup> However, since part of the effective  $k_T$  distribution is coming from higher-order QCD processes, it is clear that the distribution may be different for high- $p_T$  reactions and dimuon production. Therefore, the initial estimates obtained here are to be considered only as representative values.

The average dimuon transverse-momentum squared,  $\langle p_T^2 \rangle_{\mu\mu}$ , is, in the naive parton model, a measure of the sum of  $\langle k_T^2 \rangle$  for valence and sea quarks. Since these terms cannot be separated we shall take  $A_a = A_q$  to be the same constant for all flavors of quarks. The data of Ref. 6 show that  $\langle p_T^2 \rangle_{\mu\mu} = 1.9$  (GeV/c)<sup>2</sup> for the dimuon continuum over the range  $25 \leq Q^2 \leq 150$  (GeV/c)<sup>2</sup>. This, in turn, yields  $A_q = 1.05$  (GeV/c)<sup>-2</sup>. These same data also show that in the region of the  $\Upsilon$ ,  $9 \leq Q \leq 10.6$  GeV/c,  $\langle p_T^2 \rangle_{\mu\mu}$  is significantly larger than for the dimuon continuum. In a model for  $\Upsilon$  production<sup>22</sup> which takes into account both the quark-antiquark and gluon-gluon subprocesses, this may be interpreted as evidence that the average transverse momentum of gluons exceeds that for quarks. To see this, denote the  $q\bar{q}$  and  $gg$  contributions by  $\sigma_{q\bar{q}}$  and  $\sigma_{gg}$ , respectively, and let  $r = \sigma_{gg}/\sigma_{q\bar{q}}$ . Then,  $\langle p_T^2 \rangle_{\Upsilon}$  is a weighted average of  $\langle k_T^2 \rangle_q$  and  $\langle k_T^2 \rangle_g$ ,

$$\begin{aligned} \langle p_T^2 \rangle_{\Upsilon} &= 2(\langle k_T^2 \rangle_q + r\langle k_T^2 \rangle_g)/(1+r) \\ &= 2(A_q^{-1} + rA_g^{-1})/(1+r). \end{aligned} \quad (8)$$

The results of Ref. 22 show that for the two sets of distributions considered,  $0.50 \leq r \leq 0.67$  at  $P_{ab} = 400$  GeV/c and center-of-mass rapidity  $y = 0$ . Using  $\langle p_T^2 \rangle_{\Upsilon} = 2.3$  (GeV/c)<sup>-2</sup> and  $A_q = 1.05$  (GeV/c)<sup>-2</sup> yields  $0.65 \leq A_g \leq 0.69$  (GeV/c)<sup>-2</sup>. For

definiteness, the value  $A_g = 0.69$  (GeV/c) $^{-2}$  will be used for the remainder of this analysis.

$A_q = 1.05$  (GeV/c) $^{-2}$  corresponds to  $\langle k_T^2 \rangle = 0.95$  (GeV/c) $^2$  and  $\langle k_T \rangle = 0.86$  GeV/c. This is uncomfortably large if interpreted as being solely due to the intrinsic contribution. However, as emphasized above, this value results from an effective  $k_T$  distribution which receives contributions also from higher-order QCD processes. Therefore, this value is not incompatible with a smaller, and more realistic, contribution from the intrinsic parton transverse momentum.

### B. Subprocess cross sections

One of the distinctive features of QCD calculations of high- $p_T$  processes is that in addition to the usual  $qq$  and  $q\bar{q}$  scattering terms, there are a number of gluon related subprocesses, e.g.,  $gg \rightarrow gg$ ,  $gq \rightarrow gq$ , etc. These terms actually dominate the cross section in the intermediate- $p_T$  region. The cross sections for these various subprocesses are tabulated in Ref. 1 and may also be found in Ref. 3.

### C. Fragmentation functions

In Ref. 3 a set of fragmentation functions was determined from leptonic data for the fragmentation of quarks and gluons into  $\pi$  and  $K$  mesons. The functions were constrained to satisfy various momentum and isospin sum rules. The forms chosen for the various functions were motivated by a two-component valence (or favored) and sea (or disfavored) decomposition. In this picture the initial quark radiates gluons which, in turn, produce  $q\bar{q}$  pairs. The valence term corresponds to the situation where the initial quark combines with a member of such a gluon produced pair to form the observed  $q\bar{q}$  mesonic system. The sea term corresponds to the case where a quark and an antiquark from different gluon produced pairs combine to form the observed hadron. Thus in the sea term the initial quark does not end up in the observed hadron. It was found that fragmentation functions based on this picture and constrained by the relevant sum rules could provide a good description of the observed semi-inclusive hadron

distributions in deep-inelastic lepton scattering and  $e^+e^-$  annihilation. However, these functions were all obtained using data at low  $Q^2$ . In principle, one would expect some  $Q^2$  dependence for the fragmentation functions in analogy with the scaling deviations observed for the distribution functions. In Ref. 10 a technique for calculating such scaling deviations in fragmentation functions is presented. This technique is a straightforward extension of that which Altarelli and Parisi<sup>23</sup> used to calculate scaling deviations in parton distribution functions. It is simply based on the observation that a quark can fragment into a hadron directly, radiate a gluon before fragmenting, or radiate a gluon which fragments into the observed hadron. Similarly, a gluon can fragment into a hadron directly or it can produce a  $q\bar{q}$  or  $gg$  pair, one member of which fragments into the hadron. The result is an increase (decrease) with  $Q^2$  for  $z$  near 0 (1) in all of the fragmentation functions. This behavior is quite similar to that predicted for the distribution functions. Additional details may be found in Ref. 10.

The  $k_T$  dependence of the fragmentation functions has been taken from fits to  $e^+e^-$  annihilation data.<sup>24</sup> There a matrix element (squared) of the form  $e^{-\frac{1}{2}A^2 p_{T_i}^2}$  was used as input to a modified phase-space model for jet production. It was found that  $\langle p_T \rangle = 315$  MeV/c gave an acceptable fit. For a Gaussian  $\langle p_T \rangle = \frac{1}{2}(\pi \langle p_T^2 \rangle)^{1/2}$  so that  $\langle p_T^2 \rangle = 0.126$  (GeV/c) $^2$ . Parametrizing the fragmentation function for a parton  $c$  fragmenting into a hadron  $C$  as

$$D_{C/c}(z, \vec{k}_T) = \frac{B_c}{\pi} D_{C/c}(z) e^{-B_c k_T^2} \quad (9)$$

leads to  $B_q = 1/\langle p_T^2 \rangle = 7.94$  (GeV/c) $^{-2}$ . As in the case of the distribution functions it is assumed that all quarks have the same value for  $B_q$ . The value for  $B_g$  is obtained by setting the ratio  $B_g/B_q$  equal to  $A_g/A_q$  so that  $B_g = 5.2$  (GeV/c) $^{-2}$ .

### D. Inclusive cross section

Using the functions specified in the preceding discussion it is possible to calculate  $\pi$  and  $K$  inclusive high- $p_T$  cross sections. The full cross-section expression used here is

$$E_C \frac{d^3\sigma}{dp^3} = \sum_{a,b,c} \int \frac{dx_a}{x_{aR}} d^2k_{T_a} \frac{dx_b}{x_{bR}} d^2k_{T_b} d^2k_{T_c} x_a G_{a/A}(x_a, \vec{k}_{T_a}) x_b G_{b/B}(x_b, \vec{k}_{T_b}) D_{C/c}(z, \vec{k}_{T_c}) \frac{1}{\pi z} \frac{d\sigma}{d\hat{t}}, \quad (10)$$

where<sup>7</sup>  $x_{iR} = (x_i^2 + 4k_{T_i}^2/s)^{1/2}$ . All other notation is standard and can be found, for example, in Refs. 3 or 7. Following Ref. 9 the definition of  $Q^2$  is taken to be

$$Q^2 = \frac{2\hat{s}\hat{t}\hat{u}}{\hat{s}^2 + \hat{t}^2 + \hat{u}^2}, \quad (11)$$

where  $\hat{s}$ ,  $\hat{t}$ ,  $\hat{u}$  are the usual Mandelstam variables

for the parton-parton subprocesses. This definition has been chosen because for  $|\hat{t}| \ll \hat{s}$ ,  $|\hat{u}| \ll \hat{s}$ ,  $|\hat{t}|$ ,  $Q^2$  reduces to  $-\hat{t}$  ( $-\hat{u}$ ). Thus this definition has a  $\hat{t} \leftrightarrow \hat{u}$  symmetry which was lacking in the choice  $Q^2 = -\hat{t}$  used in Ref. 3. This symmetry is important since for  $90^\circ$  scattering in  $pp$  collisions  $\hat{u}$  is small as frequently as is  $\hat{t}$ . Thus the definition of  $Q^2$  in Eq. (11) results in a lower average  $Q^2$  than do the choices  $-\hat{t}$ ,  $(\hat{s} - \hat{t} - \hat{u})/3$ , or  $(\hat{s}\hat{t}\hat{u})^{1/3}$  discussed in Ref. 1. This lower average  $Q^2$  results in an increase in the predicted cross section. This increase then allows for the use of the scale violating fragmentation functions discussed in Sec. II C above.

As is well known, the inclusion of parton transverse momenta poses problems not encountered in the simpler purely longitudinal calculation. The smearing caused by the  $k_T$  terms allows values of  $x$  near  $x_a = x_b = 0$  to lie in the physical region. Furthermore, these  $x$  values correspond to at least one of  $\hat{s}$ ,  $\hat{t}$ , or  $\hat{u}$  being small, thereby giving rise to unphysical divergences. Of course, this region also corresponds to low values of  $Q^2$  where perturbation theory is not applicable anyway. For example, in this analysis  $\alpha_s(Q^2) = 12\pi/25 \ln(Q^2/\Lambda^2)$  with  $\Lambda^2 = 0.16$  (GeV/c) $^2$  which yields  $\alpha_s(3(\text{GeV}/c)^2) = 0.51$  and  $\alpha_s(6(\text{GeV}/c)^2) = 0.42$ . One way to reduce the effect of the divergent kinematic regions is to calculate cross sections only for  $p_T$  values such that the region  $Q^2 \leq Q_{\text{low}}^2$  is never probed. For definiteness, the value  $Q_{\text{low}}^2 = 3$  (GeV/c) $^2$  will be used. In practice this means that calculations can be performed for  $p_T \geq 3$  GeV/c at  $\sqrt{s} = 53$  GeV and  $p_T \geq 4$  GeV/c at  $\sqrt{s} = 20$  GeV. To go to lower values of  $p_T$  is meaningless since the perturbation series breaks down there. Even with this  $Q^2$  lower limit it is possible to reach the region  $x_a \approx x_b \approx 0$  by having  $k_{T_a}$  and/or  $k_{T_b}$  sufficiently large. The usual distribution functions  $G_{a/A}$  and  $G_{b/B}$  are proportional to  $1/\sqrt{x}$  or  $1/x$  for the valence or sea and gluon terms so there is again a divergence problem. This situation is handled by introducing factors of  $x_i/x_{iR}$  (Ref. 7) shown in Eq. (10). These factors effectively damp out the region of large  $k_T$  and small  $x$  so that there are no unphysical divergences.

### III. MODEL PREDICTIONS

In Figs. 1 and 2 the model predictions for high- $p_T$  inclusive pion production are compared with data<sup>25,26</sup> covering the range  $19.4 \leq \sqrt{s} \leq 62.4$  GeV and  $3 \leq p_T \leq 8$  GeV/c. The agreement between the model and the data is excellent over all of this large kinematic region. There is a tendency for the model to underestimate the  $\pi^0$  data of Ref. 26, but the agreement with the charged data,  $\frac{1}{2}(\pi^+ + \pi^-)$ ,

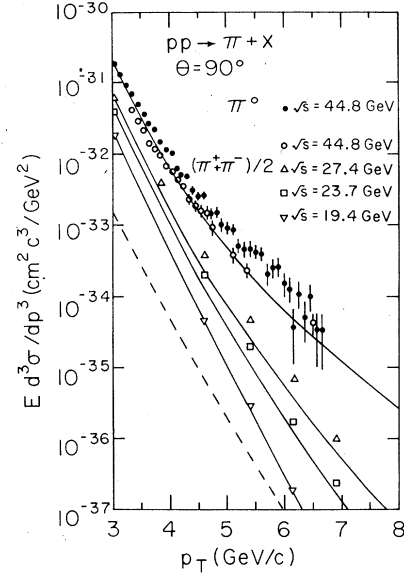


FIG. 1. Comparison of the model predictions with single-pion inclusive data (Refs. 25 and 26). The dashed curve has been calculated without the parton transverse momenta at  $\sqrt{s} = 19.4$  GeV and should be compared with the lowest solid curve.

from the same experiment is quite satisfactory. It should be noted that there is an additional 25% normalization uncertainty on the  $\pi^0$  data. The dashed curves in Figs. 1 and 2 show the results of removing the parton-transverse-momentum ef-

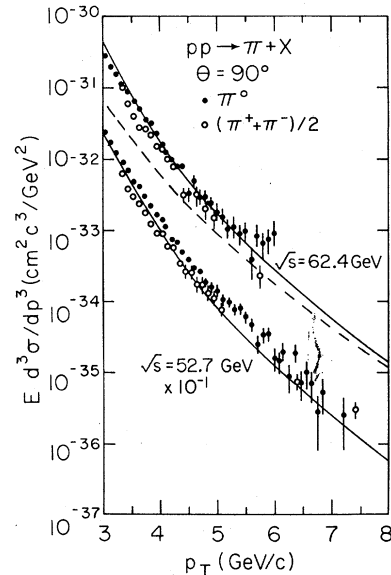


FIG. 2. Comparison of the model predictions with single-pion inclusive data (Ref. 26). The dashed curve has been calculated without the parton transverse momenta at  $\sqrt{s} = 62.4$  GeV and should be compared with the upper solid curve. Note that the data and curve at  $\sqrt{s} = 52.7$  GeV have been multiplied by a factor of 0.1.

fects at  $\sqrt{s} = 19.4$  and  $62.4$  GeV. As has been noted in previous calculations,<sup>7-9</sup> the effects of the smearing decrease at fixed  $p_T$  as  $\sqrt{s}$  increases and also decrease at fixed  $\sqrt{s}$  as  $p_T$  increases.

It is clear from these results that the lowest-order QCD calculation, augmented by the  $k_T$  smearing, is capable of describing the high- $p_T$  single-pion production data from the Fermilab through the ISR energy ranges. This may seem surprising since, naively, the QCD subprocesses are expected to give rise to a  $p_T^{-4}$  behavior at fixed  $x_T = 2p_T/\sqrt{s}$  and  $\theta$  whereas the data show a  $p_T^{-8}$  behavior. However, including the  $Q^2$  dependence of the strong running coupling constant  $\alpha_s$  together with that of the parton distribution functions has been shown to give rise to a  $p_T^{-n}$  behavior with  $n \approx 6.5$ .<sup>3</sup> Including the fragmentation function  $Q^2$  dependence raises this value further. Finally, for intermediate  $p_T$  values, the  $k_T$  smearing raises the effective value of  $n$  to values slightly greater than 8. This can best be shown<sup>9</sup> by weighting the cross section by  $p_T^8$  as shown in Fig. 3. On this plot, a model which behaved as  $p_T^{-8}$  for fixed  $x_T$  and  $\theta$  would appear as a horizontal line. For  $n > 8$  the curve falls with increasing  $p_T$  and for  $n < 8$  the curve increases with increasing  $p_T$ . Also shown in this figure are some data<sup>26</sup> which cover much of the measured kinematic region. Existing measurements do not cover the region where the model predictions show a significant rise with increasing  $p_T$ .

In Fig. 4 the model predictions for various particle production ratios are compared with the data at  $P_{lab} = 400$  GeV/c (Refs. 25 and 27) (dashed curves) and  $\sqrt{s} = 53$  GeV (Ref. 28) (solid curves). These results are qualitatively the same as those obtained in Ref. 3 and in both instances the agreement with the data is good. Quantitatively, the  $\pi^+/\pi^-$  and  $K^+/K^-$  ratios have been shifted slightly downward. This is a result of the fact that the  $gg \rightarrow gg$  and  $gq \rightarrow gq$  subprocesses are more strongly enhanced by the smearing than are the others. Therefore, the gluon fragmentation processes play a greater role and these two ratios are shifted slightly toward 1. This effect is, of course, more prominent at the lower of the two energies shown. In addition, the  $K^+/\pi^+$  ratio, which is essentially independent of energy as before, has been shifted slightly upward from 0.50 to 0.53. This shift is due to the  $Q^2$  dependence of the various fragmentation functions and is not a result of the  $k_T$  smearing.

Figures 5 and 6 show the  $\pi^0$  inclusive-cross-section predictions at  $\sqrt{s} = 19.4$  and  $62.4$  GeV, respectively, together with the contributions of the three major subprocesses. Note that the quark-quark contribution (dotted curve) contains

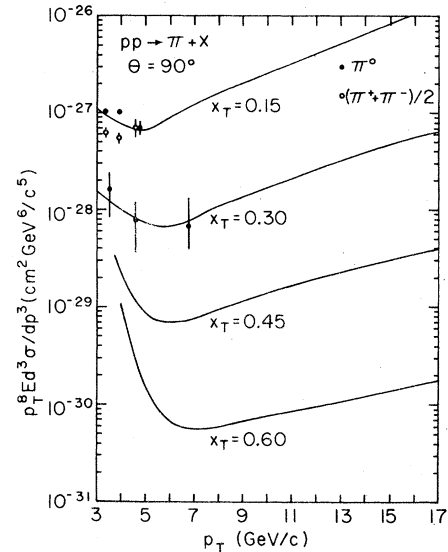


FIG. 3. Predictions for  $p_T^8 E d^3 \sigma / dp^3$  for inclusive single- $\pi^0$  production at fixed  $x_T$ . The data are from Ref. 26.

the  $q\bar{q} \rightarrow q\bar{q}$  and  $\bar{q}q \rightarrow \bar{q}q$  contributions as well. The relative sizes of the various contributions change as the energy is increased at fixed  $p_T$ . This change is due to several factors, the first of which is that at fixed  $p_T$  increasing  $s$  means decreasing  $x_T$ . Essentially, the parton distributions are probed to smaller values of  $x$ . Therefore, the

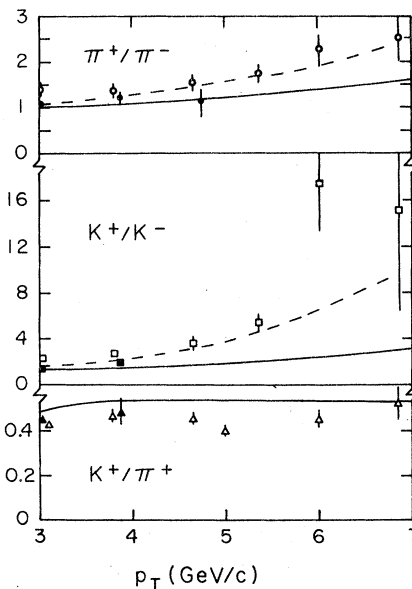


FIG. 4. Comparison of the model predictions for particle production ratios with data at  $p_{lab} = 400$  GeV/c [open symbols (Refs. 25 and 27)] and  $\sqrt{s} = 53$  GeV [closed symbols (Ref. 28)]. In each case the data are for  $pp$  reactions.

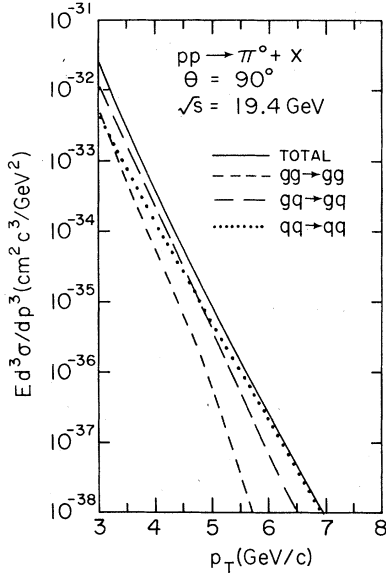


FIG. 5. Decomposition of the model prediction for inclusive single- $\pi^0$  production at  $\sqrt{s}=19.4$  GeV. Note that the  $qq \rightarrow qq$  curve includes contributions from  $q\bar{q} \rightarrow q\bar{q}$  and  $\bar{q}q \rightarrow \bar{q}q$ .

gluon-gluon term is enhanced over the gluon-quark term which, in turn, is increased more than the quark-quark term. In addition, the  $k_T$  smearing causes the steepest function of  $p_T$  to be increased the most. This effect reinforces that just described. Therefore the net effect is that at lower energies the gluon-quark contribution dominates the intermediate- $p_T$  region while at higher energies the gluon-gluon term becomes increasingly more important. Of course, eventually the gluon-

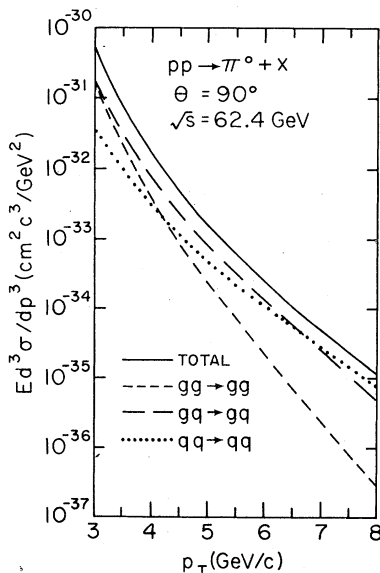


FIG. 6. Same as Fig. 5 for  $\sqrt{s}=62.4$  GeV.

gluon term is expected to dominate the intermediate- $p_T$  region.<sup>3</sup>

To date the evidence for parton-transverse-momentum smearing in high- $p_T$  inclusive reactions has primarily come from studying two-particle correlation data.<sup>4</sup> Additional evidence for such effects is becoming available from recent inclusive jet experiments.<sup>29</sup> One such experiment at Fermilab, E-395, has triggered on events where the sum of the magnitudes of the transverse momenta of the two jets is a specified constant. If all the components of each jet were detected, if no background particles were present, and if the initial partons had no transverse momenta, then the transverse momenta of the two jets would be equal and opposite and each would equal one half of the trigger value. However, experimentally, the distribution of the sum of the jet transverse momenta for a fixed trigger is smeared about the average expected value.<sup>31</sup> This smearing may be interpreted in terms of parton transverse momenta with the result that  $\langle k_T \rangle_q / \sqrt{2}$  is near 800 MeV/c and rises slowly with the  $p_T$  of the jet. This value is comparable to that observed in dimuon production, thereby lending some support to the parametrization used here.

#### IV. CONCLUSIONS

In this analysis the question of parton-transverse-momentum effects in single-particle high- $p_T$  inclusive reactions has been studied. The simple parametrization employed here presumably represents an effective  $k_T$  distribution which includes contributions from both the intrinsic parton transverse momenta as well as from higher-order QCD processes. The parameter values were estimated from dimuon production data in order to obtain some initial estimate for the size of the effects. The results of the calculations showed that the single-particle  $p_T$  distribution could be quantitatively described over a wide range in  $s$  and  $p_T$ . This range is significantly larger than is the case when the  $k_T$  effects are not included. Furthermore, the particle-production-ratio predictions are also in good agreement with the data. The calculation also demonstrates that over the kinematic region where data are currently available, the inclusive cross section has a  $p_T$  dependence at fixed  $x_T$  and  $\theta$  which goes as  $p_T^{-n}$  with  $n \approx 8-9$ . For higher energies and/or higher  $p_T$  values the value of  $n$  is expected to drop to about 6-7.

There is mounting evidence from two-particle correlation data and from inclusive jet experiments that parton-transverse-momentum effects are important for obtaining a description of the data

in the intermediate- $p_T$  range. This analysis has shown that the lowest-order QCD subprocesses are capable of describing the observed single-particle inclusive data in this region when such effects are included.

*Note added:* Another calculation of the effects of parton transverse momenta in high- $p_T$  reactions is contained in Ref. 32. This work is also

based on QCD subprocesses and the conclusions reached are similar to those obtained here and in Refs. 9 and 19.

#### ACKNOWLEDGMENT

This work was supported in part by the U. S. Department of Energy.

- 
- <sup>1</sup>B. L. Combridge, J. Kripfganz, and J. Ranft, Phys. Lett. 70B, 234 (1977).
- <sup>2</sup>R. Cutler and D. Sivers, Phys. Rev. D 17, 196 (1978).
- <sup>3</sup>J. F. Owens, E. Reya, and M. Glück, Phys. Rev. D 18, 1501 (1978).
- <sup>4</sup>M. Della Negra *et al.*, Nucl. Phys. B127, 1 (1977).
- <sup>5</sup>D. C. Hom *et al.*, Phys. Rev. Lett. 37, 1374 (1976).
- <sup>6</sup>D. M. Kaplan *et al.*, Phys. Rev. Lett. 40, 435 (1978).
- <sup>7</sup>R. P. Feynman, R. D. Field, and G. C. Fox, Nucl. Phys. B128, 1 (1977).
- <sup>8</sup>M. Fontannaz and D. Schiff, Nucl. Phys. B132, 457 (1978); F. Halzen, G. A. Ringland, and R. G. Roberts, Phys. Rev. Lett. 40, 991 (1978).
- <sup>9</sup>R. D. Field, Phys. Rev. Lett. 40, 997 (1978).
- <sup>10</sup>J. F. Owens, Phys. Lett. 76B, 85 (1978).
- <sup>11</sup>E. M. Riordan *et al.*, SLAC Report No. SLAC-Pub-1634, 1975 (unpublished); A. Bodek *et al.*, Phys. Rev. Lett. 30, 1087 (1973).
- <sup>12</sup>H. L. Anderson *et al.*, Phys. Rev. Lett. 38, 1450 (1977).
- <sup>13</sup>A. J. Buras and K. J. F. Gaemers, Nucl. Phys. B132, 249 (1978).
- <sup>14</sup>R. Blankenbecler and S. J. Brodsky, Phys. Rev. D 10, 2973 (1974).
- <sup>15</sup>H. D. Politzer, Phys. Rep. 14C, 129 (1974).
- <sup>16</sup>G. C. Fox, Nucl. Phys. B131, 107 (1977).
- <sup>17</sup>C. Sachrajda, Phys. Lett. 76B, 100 (1978).
- <sup>18</sup>Additional discussion of the effective  $k_T$  distribution may be found in Ref. 19.
- <sup>19</sup>G. C. Fox, Caltech Report No. CALT-68-643 (unpublished).
- <sup>20</sup>Detailed QCD calculations have thus far been confined primarily to dimuon-production transverse-momentum distributions. For a review see Ref. 21.
- <sup>21</sup>E. Berger, ANL Report No. ANL-HEP-PR-78-12 (unpublished).
- <sup>22</sup>J. F. Owens and E. Reya, Phys. Rev. D 17, 3003 (1978).
- <sup>23</sup>G. Altarelli and G. Parisi, Nucl. Phys. B126, 298 (1977).
- <sup>24</sup>G. Hanson, in *Deep Hadronic Structure and New Particles*, proceedings of the SLAC Summer Institute on Particle Physics, 1975, edited by Martha C. Zipf (SLAC, Stanford, 1975), p. 237.
- <sup>25</sup>D. Antreasyan *et al.*, Phys. Rev. Lett. 38, 112 (1977).
- <sup>26</sup>F. W. Büsler *et al.*, Nucl. Phys. B106, 1 (1976).
- <sup>27</sup>D. Antreasyan *et al.*, Phys. Rev. Lett. 38, 115 (1977).
- <sup>28</sup>B. Alper *et al.*, Nucl. Phys. B87, 19 (1975).
- <sup>29</sup>For a review see Ref. 30.
- <sup>30</sup>G. C. Fox, in *Particles and Fields—1977*, Proceedings of the Meeting of the APS Division of Particles and Fields, edited by P. A. Schreiner, G. H. Thomas, and A. B. Wicklund (AIP, New York, 1978), p. 193.
- <sup>31</sup>A. R. Erwin, talk presented at the 1978 Vanderbilt Conference, Report No. COO-088-36, 1978 (unpublished).
- <sup>32</sup>A. P. Contogouris, R. Gaskill, and S. Papadopoulos, Phys. Rev. D 17, 2314 (1978).